Society For Biomaterials

# Biomechanical characterization of a novel collagen-hyaluronan infused 3D-printed polymeric device for partial meniscus replacement

**Salim A. Ghodbane,[1,2] Jay M. Patel,[1,2] Andrzej Brzezinski,[1] Tyler M. Lu,[1] Charles J. Gatt,[1,2] Michael G. Dunn[1,2]**

[1]Department of Orthopaedic Surgery, Rutgers Biomedical and Health Sciences - Robert Wood Johnson Medical School, New Brunswick, New Jersey, USA
[2]Department of Biomedical Engineering, Rutgers, The State University of New Jersey, Piscataway, New Jersey, USA

Received 14 May 2018; revised 8 December 2018; accepted 26 January 2019
Published online 00 Month 2019 in Wiley Online Library (wileyonlinelibrary.com). DOI: 10.1002/jbm.b.34336

**Abstract:** The menisci transmit load by increasing the contact area and decreasing peak contact stresses on the articular surfaces. Meniscal lesions are among the most common orthopedic injuries, and resulting meniscectomies are associated with adverse polycaprolactone contact mechanics changes and, ultimately, an increased likelihood of osteoarthritis. Meniscus scaffolds were fabricated by 3D-printing a network of circumferential and radial filaments of resorbable polymer (poly(desaminotyrosyl-tyrosine dodecyl ester dodecanoate)) and infused with collagen-hyaluronan. The scaffold demonstrated an instantaneous compressive modulus (1.66 $\pm$ 0.44 MPa) comparable to native meniscus (1.52 $\pm$ 0.59 MPa). The scaffold aggregate modulus (1.33 $\pm$ 0.51 MPa) was within 2% of the native value (1.31 $\pm$ 0.36 MPa). In tension, the scaffold displayed a comparable stiffness to native tissue (127.6–97.1 N/mm) and an ultimate load of 33% of the native value. Suture pull-out load of scaffolds (83.1 $\pm$ 10.0 N) was within 10% of native values (91.5 $\pm$ 15.4 N). Contact stress analysis demonstrated the scaffold reduced peak contact stress by 60–67% and increased contact area by 38%, relative to partial meniscectomy. This is the first meniscal scaffold to match both the axial compressive properties and the circumferential tensile stiffness of the native meniscus. The improvement of joint contact mechanics, relative to partial meniscectomy alone, motivates further investigation using a large animal model. © 2019 Wiley Periodicals, Inc. J Biomed Mater Res Part B: 00B: 000–000, 2019.

**Key Words:** knee, meniscus, tissue engineering, biomaterials

**How to cite this article:** Ghodbane SA, Patel JM, Brzezinski A, Lu TM, Gatt CJ, Dunn MG. 2019. Biomechanical characterization of a novel collagen-hyaluronan infused 3D-printed polymeric device for partial meniscus replacement. J Biomed Mater Res Part B. 2019:9999B:1–9.

## INTRODUCTION

The menisci of the knee are semilunar fibrocartilaginous structures localized between the femoral condyle and tibial plateau, and are integral to load transmission, joint stabilization, and shock absorption of the knee.[1,2] The form of the menisci, characterized by a concave superior surface and a flat inferior surface, is crucial to its biomechanical function, transmitting 50–85% of the compressive loads of the knee joint.[3] This unique shape allows the menisci to increase the contact area between the curved femoral condyle and the tibial plateau.[4] By increasing the congruency of the articular surfaces, the menisci can prevent high contact stresses from being imposed upon the underlying articular cartilage.[5]

Meniscal lesions are among the most common orthopedic injuries given the significant stresses imposed upon the tissue.[6] While meniscal repair is successful in the outer, vascularized region of the meniscus, the only treatment for meniscal lesions within the inner body is partial meniscectomy. This procedure has been shown to provide short-term symptom relief[7]; however, there is a direct correlation between the amount of meniscectomized tissue and the risk of osteoarthritis.[8] The degeneration of the articular cartilage is likely the result of increased peak contact stresses and reduced contact area on the cartilage.[9]

Allograft transplantation is an option following total meniscectomy, but suffers from the issues of limited availability, disease transmission, immune rejection, and anatomical mismatching.[10] In addition, although the initial mechanics are appropriate, the dense tissue is not easily remodeled, resulting in poor and inconsistent long-term outcomes.[11] Therefore, there is significant interest in developing off-the-shelf devices for meniscal replacement.

Two resorbable devices have been used in clinical trials for partial meniscus replacement: the collagen meniscus implant (CMI), composed of cross-linked bovine-derived collagen, and Actifit, composed of polyester-urethane. Although

**Correspondence to:** M. G. Dunn; e-mail: dunnmg@rwjms.rutgers.edu
Contract grant sponsor: Armed Forces Institute for Regenerative Medicine II; contract grant number: W81XWH-08-2-0034
Contract grant sponsor: National Institute of General Medical Sciences; contract grant number: T32 GM8339

CMI was developed decades ago, the device is yet to be widely adopted and is not reimbursed by Medicare.[12] Actifit has exhibited poor survivorship, with 36.4% requiring removal in a recent clinical trial.[13] Other researchers have attempted to develop homogenous, tissue-engineered scaffolds composed of biologic and/or synthetic materials.[14–23] However, these scaffolds are limited by their isotropic structure, which do not properly mimic the function of the anisotropic meniscus.

An anisotropic structure is necessary to replicate the mechanical function of the meniscus. Additionally, anisotropic scaffolds result in improved cellular and extracellular matrix (ECM) alignment, increased ECM deposition, and an increased rate of mechanical improvement.[23–27] Groups have attempted to recreate the anisotropy of the native meniscus utilizing fabrication techniques such as weaving,[28] electrospinning,[29] or 3D-printing.[19,30] However, these devices have never successfully matched the mechanics of the native meniscus in both compression and tension, and fewer have demonstrated the ability to reduce contact stresses on the cartilage under compressive loading.[17,31]

A resorbable *total* meniscus replacement scaffold composed of a woven poly(desaminotyrosyl-tyrosine dodecyl ester dodecanoate) [poly(DTD DD)] fiber reinforced collagen-hyaluronan (COL-HA) sponge was previously developed.[32–34] The scaffold was designed to match the circumferential tensile and axial compressive mechanics of the native ovine meniscus with appropriate porosity (>70%[35]) for tissue infiltration. The poly(DTD DD) architecture mimics the native organization of the collagen fibers in the meniscus with successive layers of circumferential and radial filaments and provides the mechanics of the scaffold (Figure 1). A COL-HA sponge is infused into the voids of the 3D printed polymer to provide a biological substrate for infiltrating cells.

The scaffold filament density (i.e., the number of fibers per layer) and 3D-printing parameters (i.e., print temperature, print speed, print nozzle diameter, etc.) were optimized specifically to match the axial compressive properties and circumferential tensile stiffness of the native ovine meniscus. The ultimate tensile load of the scaffold was not part of the design criteria, considering the indication for a partial meniscus scaffold includes an intact peripheral rim, which performs the majority of the circumferential tensile function of the native meniscus.[9,36]

In this study, we evaluated a resorbable collagen-hyaluronan infused 3D-printed poly(DTD DD) scaffold that could be cut into various sizes and shapes for *partial* meniscus replacement. Our objective was to design and fabricate a partial meniscus scaffold that could (1) match the axial compressive properties and (2) circumferential tensile stiffness of the native ovine meniscus, (3) possess adequate suture retention properties, and (4) restore functional contact mechanics of the ovine stifle joint relative to an 80% meniscectomy.

## METHODS

The meniscus scaffold design was fabricated and tested for the following: axial compressive properties, circumferential tensile properties, and suture retention properties. All comparisons were made to fresh frozen ovine medial menisci (skeletally mature, ages 4–8 years old), acquired from Colorado State University. Once the scaffold mechanics were established, the scaffold's ability to limit contact stresses in the knee was evaluated *in situ* and compared to intact meniscus, autograft, and 80% meniscectomy conditions.

### Scaffold design and fabrication

Poly(DTD DD) was 3D printed at 160°C at 1.2 mm/s at 8.9 bar with a 400 μm inner diameter needle on a 3D Bioplotter (EnvisionTEC, Dearborn, MI) at the New Jersey Center for Biomaterials (Department of Chemistry, Rutgers University, Piscataway, NJ). The scaffolds were printed with an anterior–posterior length of 32 mm and a medial–lateral length of 24 mm. Sodium hyaluronate (0.25 g/L; molecular weight 1.5–2.2 MDa, Acros Organic, Bridgewater, NJ) was dissolved in dilute hydrochloric acid (pH 2.35). Lyophilized bovine Achilles tendon collagen (Worthington Biochemical Corporation, Lakewood, NJ) was ground and swollen in the acidic solution (20 g/L), adapted from previous methods.[21,32,37,38] The scaffolds were infused with COL-HA, frozen, and lyophilized. The collagen within the scaffolds were cross-linked with 10 mM, 1-ethyl-3-(3-dimethaylaminopropyl)carbodiimide hydrochloride and 5 mM *N*-hydroxysuccinimide for 6 h. Scaffolds were rinsed three times for 10 min in DI water, once for 3 h in 100 mM sodium phosphate, and rinsed for 24 h in DI water. Scaffolds were frozen, lyophilized, and sterilized with 25 kGy of gamma irradiation (Sterigenics, Rockaway, NJ) [Figure 1(D)].

### Scaffold properties

The 3D-printed polymer network was visually inspected then weighed after printing (polymer weight). The scaffold was weighed after all fabrication steps including COL-HA infusion (total weight). The percent polymer and percent COL-HA were calculated from these values.

Scaffold porosity was determined via an ethanol infiltration assay.[39] A 4-mm-diameter biopsy punch was removed from dry scaffolds ($n$ = 6) and trimmed to obtain a cylindrical sample. The height was measured using Vernier calipers and the dry mass was measured ($m_{\mathrm{dry}}$). The samples were soaked in 100% ethanol for 1 h, superficially dried, and the mass was immediately measured ($m_{\mathrm{e}}$). The porosity was found by dividing the pore volume by the total volume, as demonstrated by the following equation:

$$\%\text{porosity} = \frac{m_{\mathrm{e}} - m_{\mathrm{dry}}}{\rho V} \times 100\%$$

where $\rho$ represents the density of ethanol (0.789 mg/mL) and $V$ represents the volume of the sample.

### Confined compressive creep

Cylindrical plugs of 4 mm diameter and 3 mm height were taken from the anterior, body, and posterior regions of scaffolds and native menisci ($n$ = 12, 4 × 3 regions) and hydrated in phosphate-buffered saline (PBS) at room temperature for at least 1 h. The hydrated plugs were placed in

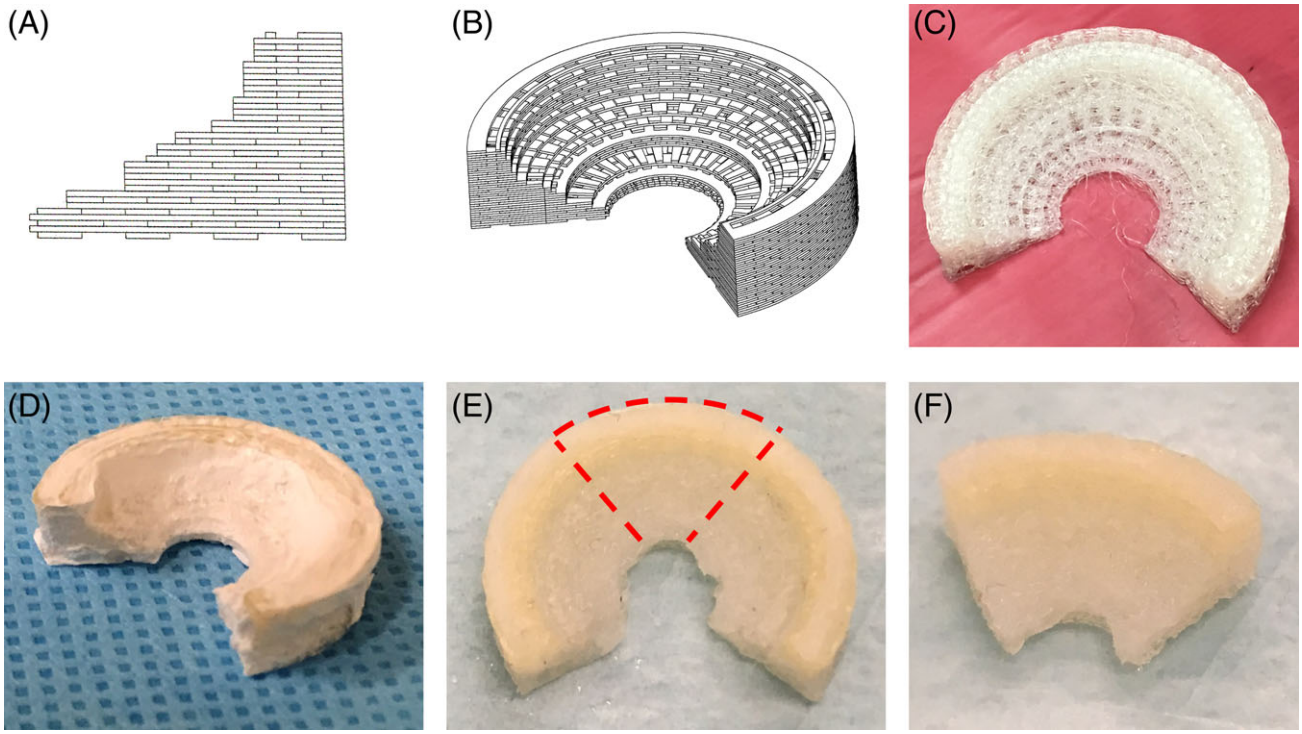


**FIGURE 1.** Scaffold computer aided design: (A) cross-section and (B) 3D view. C: Polymer scaffold prior to infusing with COL-HA. D: COL-HA infused, sterilized partial meniscus scaffold. E: Hydrated scaffold with red dotted lines indicating cutting lines. F: Resulting cut scaffold for 80% partial meniscus replacement in ovine knees.

a 4-mm-diameter cylindrical stainless-steel chamber with a porous stainless-steel unidirectional fluid flow filter. A 1 N load was applied for 3600 s (model 5542; Instron, Canton, MA). The instantaneous compressive modulus was calculated from the initial loading phase from 0.5 to 1 N. The aggregate moduli and permeability of the samples were calculated according to Mow's biphasic theory.[40]

### Circumferential tensile testing

Scaffolds and native menisci ($n$ = 6/group) were hydrated in PBS at room temperature for at least 1 h. Each scaffold or meniscus was loaded into cryogenic freeze clamps (TA Instruments, New Castle, DE) with an 8 mm gage length encompassing the central region. The samples were loaded in tension at a rate of 10 mm/min to failure (model 5592; Instron, Canton, MA). Circumferential tensile stiffness and ultimate tensile load were calculated for each sample. Circumferential tensile stiffness was defined as the steepest portion of the load–deformation curve. Ultimate tensile load was defined as the maximum load observed before failure.

### Suture retention testing

Suture retention testing was performed on hydrated scaffolds and native menisci ($n$ = 6 each). A 2-0 Ethibond suture was placed radially in a vertical mattress fashion, 2 mm from the outer margin of samples. Two gripping sutures were placed through the sample on either side of the Ethibond suture, reinforced with cardiovascular pledgets (Ethicon, Somerville, NJ), and looped around the outer margin [Figure 5(A,B)]. The sutures were looped around pins connected to each end of the instron. The Ethibond suture was loaded in tension at 50 mm/min until failure.[10,41] Mode of failure was recorded, and the fixation stiffness and pull-out load were calculated. Fixation stiffness was defined as the steepest portion of the load–deformation curve. Pull-out load was defined as the maximum load observed before failure.

### Contact stress testing

Fresh frozen ovine hind limbs with varying sized menisci (skeletally mature, 4–8 years old) were obtained from Colorado State University ($n$ = 6). The limbs were thawed, and the skin, subcutaneous fat, muscle, and patella were removed, taking care to preserve the cruciate ligaments, collateral ligaments, and capsule. The tibia and femur were transected about 3 cm below and 10 cm above the joint line, respectively. The tibia was potted in polymethylmethacrylate and allowed to cure for 30 min. Bone tunnels were drilled in the femur at 0° and 30° flexion, allowing for natural rotation and varus–valgus alignment of the femoral condyles at each angle, to allow for mounting of the specimen.

All joints were inspected prior to testing for signs of meniscal or cartilage damage. For testing, the anterior and posterior capsules were transected just under the medial meniscus to allow for insertion of a pressure-sensitive sensor (K-Scan #4000, Tekscan Inc.). The Tekscan strip was trimmed to the width of the medial compartment and covered in Tegaderm Transparent Film (3M, St. Paul, MN). The medial collateral ligament (MCL) was released at the femoral

attachment to access the medial compartment and reattached with a suture endobutton technique (Smith and Nephew, Andover, MA) [Figure 2(A,B)]. Prior to testing, the Tekscan strip was preconditioned five times at 1500 N, and calibrated at 250 N and 1000 N. The strip was covered in petroleum jelly, a suture was placed through the leading edge of the strip, and the suture was pulled to place the strip under the medial meniscus[42] [Figure 2(D)].

The knee was loaded into a custom jig in an Instron (model 5592; Instron, Canton, MA), maintaining natural alignment of the joint [Figure 2(F)]. Following hydration, a 200 N load was applied at a deformation rate of 30 mm/min on the medial compartment for 5 cycles of preconditioning followed by 15 cycles of testing. The peak contact pressure, mean contact pressure, and contact area were calculated for each cycle and averaged for each knee in MATLAB (R2015b, Mathworks, Natick, MA). The knee was tested in the following order: the intact meniscus, partial autograft, scaffold, and 80% (measured in relation to the meniscal radial width) posterior partial meniscectomy [Figure 2(C,E)]. To perform these tests, following the intact condition, the meniscectomy was performed and the meniscectomized tissue was sutured into anatomical position for the autograft condition. Once tested, the autograft was removed, and the scaffold was implanted and tested. Finally, the scaffold was removed for the meniscectomy condition. Although partial autograft does not represent a realistic clinical option, it provides a positive control with the ideal material properties of the native meniscus. The autograft and scaffold were sutured with 2-0 Ethibond sutures (Ethicon, Somerville, NJ) with two running radially and two circumferentially.

### Statistical analysis

A Student's $t$ test was performed to compare the confined compressive creep, circumferential tension, and suture retention testing between native ovine meniscus and the scaffold. A repeated-measures analysis of variance (ANOVA) with a post-*hoc* Sidak's test was performed for the contact stress analysis. For all tests, statistical significance was defined as $p < 0.05$ and performed using Minitab v 17.

## RESULTS

### Scaffold properties

A total of 24 scaffolds were successfully fabricated with high print fidelity for partial meniscus replacement [Figure 1(C)]. The average print time was 142 $\pm$ 3 min. The total scaffold mass was 541 $\pm$ 70 mg with a polymer mass of 499 $\pm$ 59 mg and a COL-HA mass of 42 $\pm$ 22 mg, corresponding to an average of 92% polymer and 8% COL-HA by weight. The scaffold porosity was 69.9 $\pm$ 8.0%.

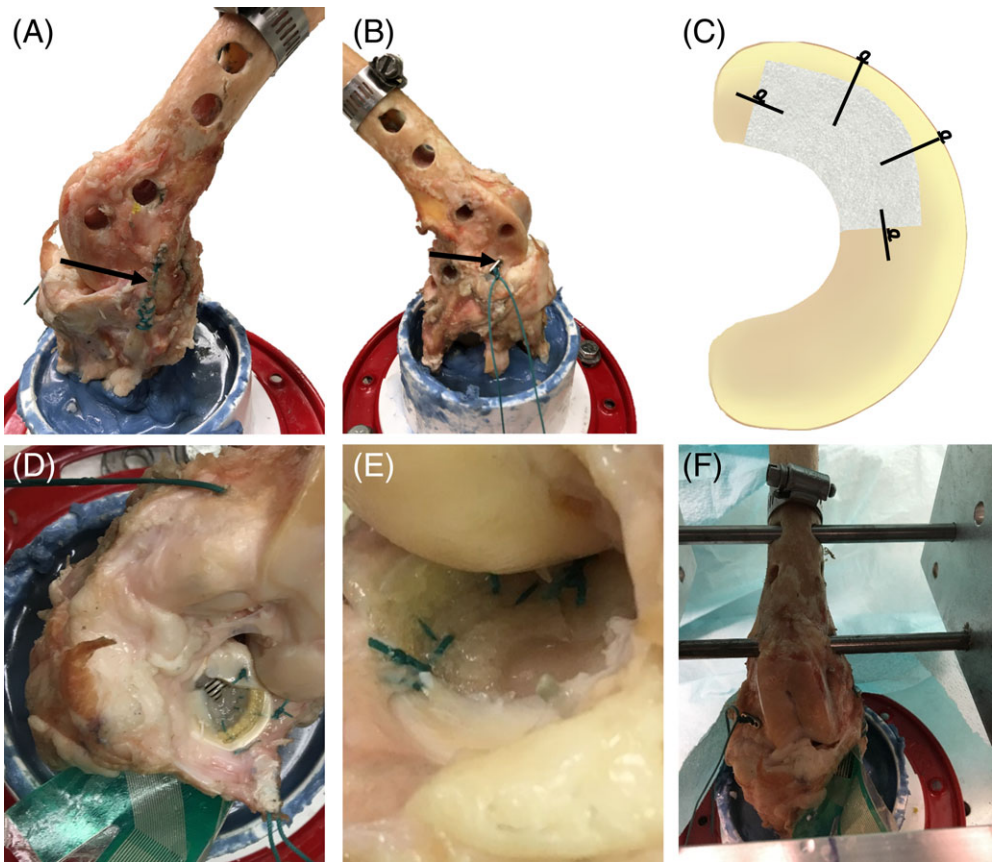


**FIGURE 2.** (A) Sutured MCL attachment and (B) endobutton fixation of MCL for contact stress testing. C: Scaffold fixation scheme with lines representing 2-0 Ethibond sutures. Suture knot locations are depicted by loops. D: Tekscan strip placed underneath meniscus for tibial pressure measurements. E: Scaffold sutured into defect site. F: Ovine knee specimen mounted in mechanical testing machine.

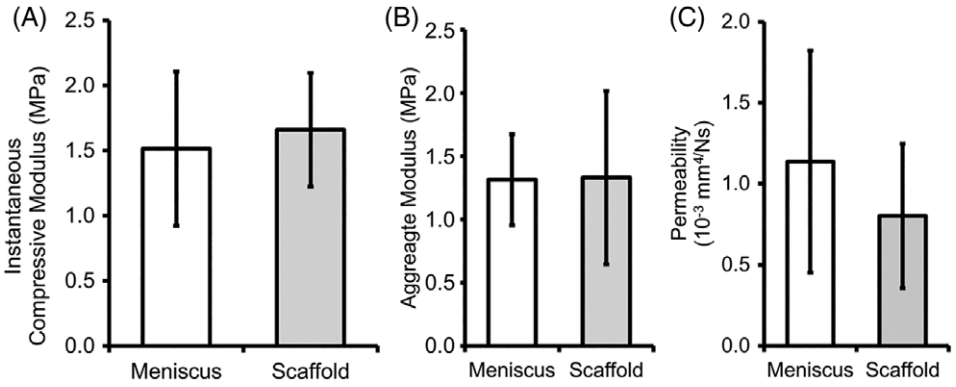


**FIGURE 3.** (A) Instantaneous compressive modulus, (B) aggregate modulus, and (C) permeability of native ovine meniscus and scaffold ($n$ = 4 from the anterior, body, and posterior regions). The values indicated represent mean ± SD.

### Scaffold mechanics

The scaffold closely matched both the instantaneous and time-dependent compressive properties of the native meniscus (Figure 3). The instantaneous compressive modulus of the scaffold (1.66 ± 0.44 MPa) and native meniscus (1.52 ± 0.59 MPa) were comparable ($p$ = 0.26). The aggregate modulus of the scaffold (1.33 ± 0.51 MPa) was within 2% of the native meniscus (1.31 ± 0.36 MPa) and not significantly different ($p$ = 0.93). The permeability of the scaffold was lower, but this difference was not statistically significant ($p$ = 0.075). The tensile stiffness of the scaffold (127.6 ± 47.6 N/mm) was 31.4% greater ($p$ = 0.953) than that of the native ovine meniscus (97.1 ± 40.3 N/mm) (Figure 4). The ultimate tensile load of the scaffold was 33% of that of the native meniscus ($p$ < 0.01).

In suture retention testing, the suture pulled out of the scaffold 6 out of 6 samples, whereas for the native meniscus, the suture failed in 4 samples and the suture pulled out of 2. The scaffold (83.1 ± 10.0 N) possessed a similar ultimate pull-out load ($p$ = 0.25) to the native meniscus (91.5 ± 15.4 N) [Figure 5 (C)]. The mean stiffness of the scaffold fixation was 30% less than that of the native meniscus ($p$ < 0.01) [Figure 5(D)].

### Contact stress testing

Angle of flexion did not affect the contact mechanics of the ovine stifle joint for any condition ($p$ = 0.988). Relative to partial meniscectomy, the scaffold significantly reduced peak contact stress by 60–67% and increased contact area by 138% (Figures 6 and 7). Partial meniscectomy demonstrated significantly greater peak and mean contact stress and significantly less contact area than all other conditions. Compared to the intact condition, the joint experienced progressive increases in peak contact stresses of 20%, 45%, and 130% and mean contact stress of 7%, 18%, and 167%, for autograft, scaffold, and meniscectomy, respectively. Likewise, the contact area successively decreased by 6%, 16%, and 40%, respectively. The scaffold performed equivalently to autograft for mean contact stress ($p$ = 0.079) and peak contact stress ($p$ = 0.103) with a 9–12% significantly reduced contact area ($p$ = 0.001). The region of peak stress appeared to be more centrally located in the scaffold group compared to the intact and autograft conditions, for which the peak stress was more anterior.

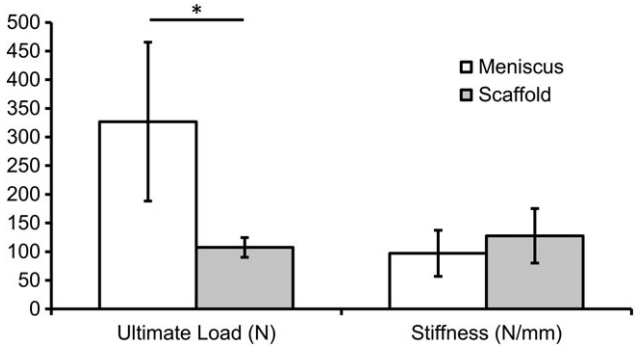


**FIGURE 4.** Ultimate tensile load and tensile stiffness of scaffold compared with native ovine menisci ($n$ = 6/group). The values indicated represent mean ± SD. * denotes statistically significant difference ($p$ < 0.05).

## DISCUSSION

The primary mechanical function of the meniscus is to transmit and distribute joint loads to protect the tibial and femoral articular cartilage. The meniscus is capable of performing this function due to its complex microstructure and resulting anisotropic mechanical properties. This study demonstrates an acellular, off-the-shelf, resorbable 3D-printed COL-HA infused polymeric scaffold could approximate key structural properties of the native ovine meniscus and restore load-distribution properties, following partial meniscectomy, of the ovine knee joint. The scaffolds maintained their structural integrity after being cut into different geometries required for the various mechanical testing methods, and for the 80% meniscectomy defect model, an essential characteristic for partial meniscus replacement. If the combined biomechanical properties of the scaffold with the neo-meniscal tissue can be maintained, during long-term implantation, this scaffold has the potential to delay, or possibly prevent, the onset of osteoarthritis caused by partial meniscectomy.

Compressive properties are integral to the load-sharing properties of meniscus devices. An overly stiff device will be overloaded, causing stress concentrations on the cartilage. A device which is not stiff enough may not be adequately loaded or may potentially collapse or shrink, as reported in human studies of CMI.[43] In addition, scaffolds with compressive

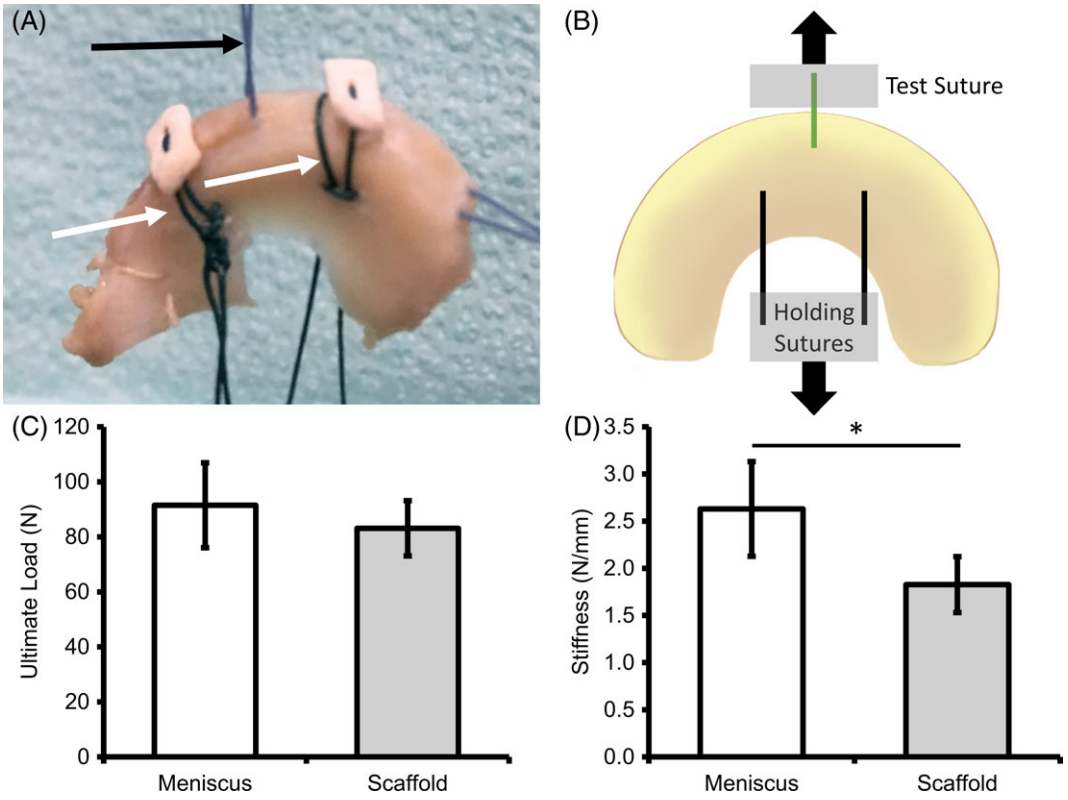


**FIGURE 5.** (A) Representative image of vertical mattress suture retention testing. Black arrow points to the tested suture and white arrows indicate gripping suture. Direction of testing is vertical. B: Schematic of testing setup. C: Pull-out ultimate load and (D) fixation stiffness of native ovine meniscus and scaffold. The values indicated represent mean ± SD. * denotes statistically significant difference ($p < 0.05$).

moduli that closely match those of the native meniscus induce greater fibrocartilage formation.[44] To our knowledge, this is the first partial meniscus device to successfully replicate the compressive properties of the native ovine meniscus. Others have achieved less than half of the compressive properties of the native meniscus.[15,19] CMI and Actifit possess compressive properties of about 25% of ovine meniscus and 26–27% of the human meniscus.[45]

Tensile mechanics are also integral to the load-sharing properties. Our 3D-printed scaffold demonstrated a comparable circumferential stiffness of the native meniscus (131.3%) with a significantly lower ultimate load (107 N). However, ultimate load was not included in our design criteria for a successful scaffold, because the indication for a partial meniscus scaffold requires an intact peripheral rim and the maximum expected circumferential load experienced by an ovine meniscus is estimated to be ~120 N.[46–48] There are no other partial meniscal devices that have tensile properties that approach native meniscus values. Tensile stiffness of scaffolds in the literature range from 25–47% of native meniscus values using a variety of fabrication techniques.[19,45] For example, the tensile stiffness of CMI and Actifit are 42% and 25% that of native ovine meniscus values, respectively.[45] Lee et al. reported a 3D printed polycaprolactone (PCL) scaffold that possessed a tensile modulus of 47% and an ultimate strength of 57% of the native ovine meniscus.[19]

With compressive properties and tensile stiffness similar to native tissue, the suture retention properties of our scaffold were established to validate the ability to implant the device. The pull-out strength is important for surgeon handling and positioning of the scaffold during implantation. The vertical mattress suture has been well documented as the strongest suturing repair technique[41,49,50] and thus was used in our suture retention study. Pull-out load and stiffness of our scaffold were 90.8% and 69.5% of native meniscus, respectively. Similarly, Lee et al. found that the pull-out load of their 3D-printed scaffold was comparable to that of the native meniscus.[19] Interestingly, the pull-out strength of CMI is only ~20 N[51] and that of Actifit is 50 N,[52] with no suture pull-out problems reported clinically, suggesting that the pull-out strength of our scaffold (83 N) is more than sufficient for clinical use.

The aforementioned mechanical parameters all contribute to the device's ability to distribute loads in the joint. In this study, we were able to demonstrate restoration of contact area and reduction of contact stresses by implanting the device following partial meniscectomy. An 80% partial meniscectomy resulted in a 40% decrease in contact area and a 130% increase in peak contact stress. The observed change in contact area was in agreement with previous contact stress analyses of meniscectomized knees (i.e., 34–58% decrease in contact area).[9,31,36,42,53–55] However, those previous studies observed peak contact stress increases of only

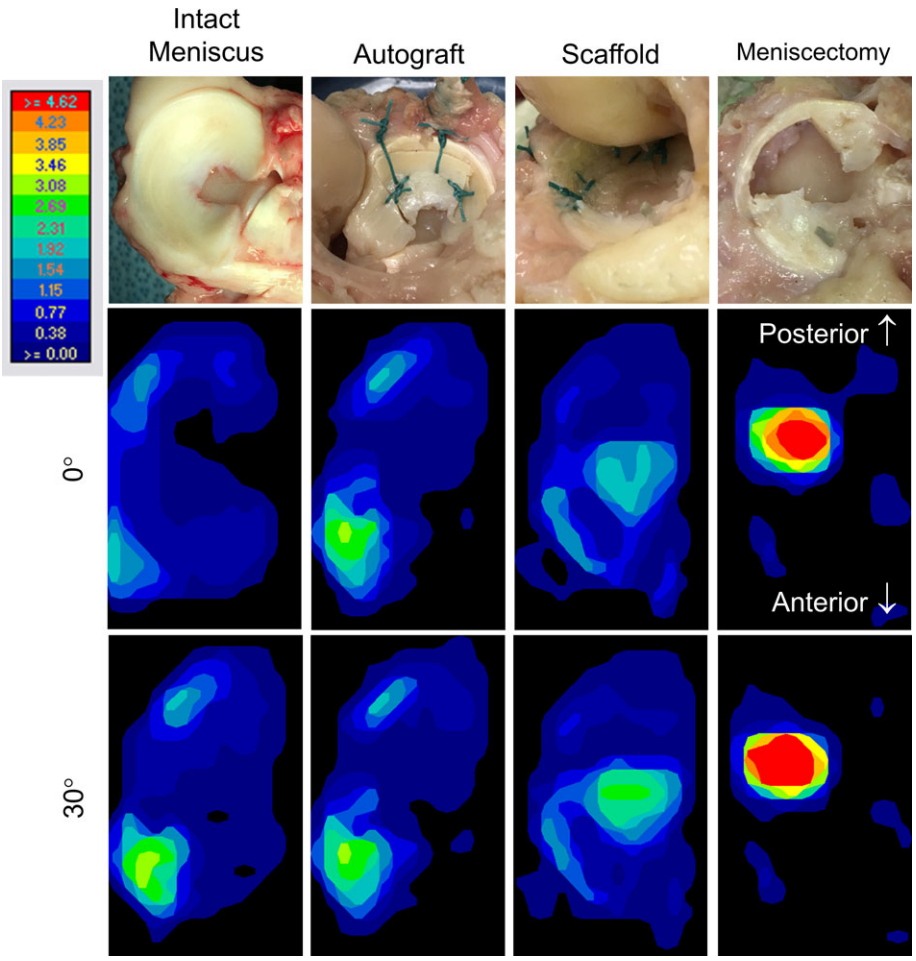


**FIGURE 6.** Representative images of intact meniscus, autograft, scaffold, and partial meniscectomy conditions. Pressure maps for each condition at 0° and 30° flexion, scaled from 0 to 4.62 MPa.

58–77%; our 130% increase may be a result of the size (80% resection) of our partial meniscectomy model. Moreover, peak contact stresses with the implanted scaffold were only 22% greater than autograft, indicating that our scaffold performs comparably to native meniscal tissue sutured back to the outer rim.

To our knowledge, the only previous assessment of a scaffold's ability to restore contact stresses in the knee involved Actifit.[31,56] In these studies, Actifit restored mean contact pressure to intact levels, but peak contact pressure increased by 36% and contact area decreased by 20%, relative to the intact knee, similar to the results with our scaffold. Unlike these previous studies, this study used a posterior partial meniscectomy, which may represent a more clinically relevant model.[57,58] Moreover, this is the first study to assess an autograft to provide a positive control for comparison to a partial meniscus scaffold.

This study was not without limitations. Material properties were not calculated for the tensile properties due to difficulties measuring the cross-sectional area of native meniscus specimens. However, it may be more appropriate to compare the structural properties, considering the initially oversized scaffold is compressed to conform to the remaining meniscus. For the contact stress analysis, 60° flexion was not tested due to limitations with the testing jig; nonetheless, no effect was found regarding flexion angle for the two conditions tested.

In conclusion, we designed, fabricated, and tested a partial meniscus replacement scaffold which replicates both the axial compressive properties and circumferential tensile stiffness of the native ovine meniscus and demonstrated that the scaffold could retain sutures to clinically sufficient loads. Furthermore, by implanting this scaffold into an 80% partial resection model, we demonstrated the ability of this scaffold to restore near-normal cartilage contact stresses. The implanted scaffold significantly reduced peak contact stresses, mean contact stresses, and increased contact area relative to partial meniscectomy. This scaffold was designed and fabricated for the ovine meniscus, and there are significant anatomical and mechanical similarities between the human and ovine menisci[59]; therefore, the design can be easily translated to the human meniscus with only minor alterations. A scaffold possessing these structural and biomechanical characteristics has the potential to restore knee function and prevent osteoarthritis in patients with severe meniscal injuries or meniscectomies. These results warrant

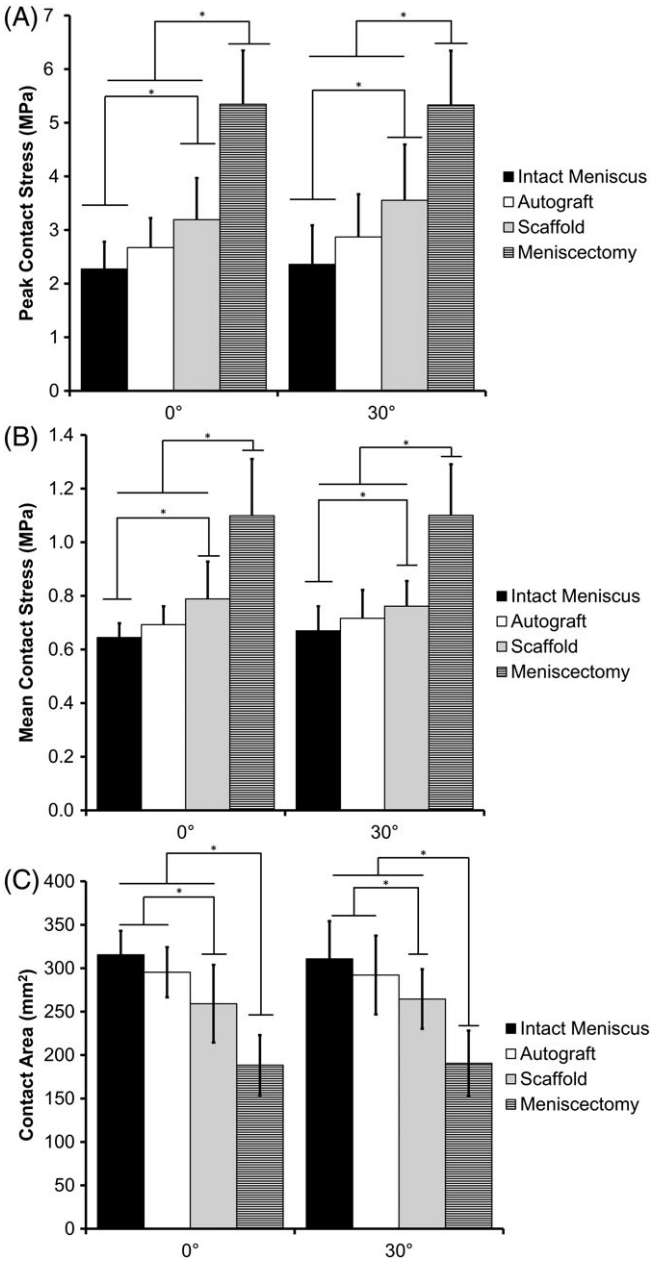


**FIGURE 7.** (A) Peak contact stress, (B) mean contact stress, and (C) contact area for intact meniscus, autograft, scaffold, and partial meniscectomy conditions at 0° and 30° flexion. The values indicated represent mean ± SD. * denotes statistically significant difference ($p < 0.05$).

further investigation of the functional and chondroprotective abilities of these scaffolds in a large animal partial meniscus replacement model.[60]

## REFERENCES


1. Makris EA, Hadidi P, Athanasiou KA. The knee meniscus: Structure-function, pathophysiology, current repair techniques, and prospects for regeneration. Biomaterials 2011;32(30):7411–7431.
2. Fithian DC, Kelly MA, Mow VC. Material properties and structure-function relationships in the menisci. Clin Orthop Relat Res 1990; 252:19–31.
3. Ahmed AM, Burke DL. In-vitro measurement of static pressure distribution in synovial joints-Part I: Tibial surface of the knee. J Biomech Eng 1983;105(3):216–225.
4. Shaffer B, Kennedy S, Klimkiewicz J, Yao L. Preoperative sizing of meniscal allografts in meniscus transplantation. Am J Sports Med 2000;28(4):524–533.
5. Fox AJ, Bedi A, Rodeo SA. The basic science of human knee menisci: Structure, composition, and function. Sports Health 2012;4 (4):340–351.
6. Sihvonen R, Paavola M, Malmivaara A, Itala A, Joukainen A, Nurmi H, Kalske J, Jarvinen TL, Finnish Degenerative Meniscal Lesion Study Group. Arthroscopic partial meniscectomy versus sham surgery for a degenerative meniscal tear. N Engl J Med 2013; 369(26):2515–2524.
7. Northmore-Ball MD, Dandy DJ, Jackson RW. Arthroscopic, open partial, and total meniscectomy. A comparative study. J Bone Joint Surg (Br) 1983;65(4):400–404.
8. Papalia R, Del Buono A, Osti L, Denaro V, Maffulli N. Meniscectomy as a risk factor for knee osteoarthritis: A systematic review. Br Med Bull 2011;99(1):89–106.
9. Lee SJ, Aadalen KJ, Malaviya P, Lorenz EP, Hayden JK, Farr J, Kang RW, Cole BJ. Tibiofemoral contact mechanics after serial medial meniscectomies in the human cadaveric knee. Am J Sports Med 2006;34(8):1334–1344.
10. Fisher SR, Markel DC, Koman JD, Atkinson TS. Pull-out and shear failure strengths of arthroscopic meniscal repair systems. Knee Surg Sports Traumatol Arthrosc 2002;10(5):294–299.
11. Noyes FR, Barber-Westin SD. Long-term survivorship and function of meniscus transplantation. Am J Sports Med 2016;44(9):2330–2338.
12. Department of Health & Human Services (DHHS). Change Request 6903. Baltimore, MD: Centers for Medicare & Medicaid Services; 2010.
13. Van Der Straeten C, Doyen B, Dutordoir C, Goedertier W, Pirard S, Victor J. Short- and medium-term results of artificial meniscal implants. Orthopaed Proc 2016;98-B(SUPP 4):91–91.
14. Puetzer JL, Bonassar LJ. High density type I collagen gels for tissue engineering of whole menisci. Acta Biomater 2013;9(8):7787–7795.
15. Gruchenberg K, Ignatius A, Friemert B, von Lubken F, Skaer N, Gellynck K, Kessler O, Durselen L. In vivo performance of a novel silk fibroin scaffold for partial meniscal replacement in a sheep model. Knee Surg Sports Traumatol Arthrosc 2015;23(8):2218–2229.
16. Koller U, Nehrer S, Vavken P, Kapeller B, Windhager R, Chiari C. Polyethylene terephthalate (PET) enhances chondrogenic differentiation of ovine meniscocytes in a hyaluronic acid/polycaprolactone scaffold in vitro. Int Orthop 2012;36(9):1953–1960.
17. Maher SA, Rodeo SA, Doty SB, Brophy R, Potter H, Foo LF, Rosenblatt L, Deng XH, Turner AS, Wright TM, Warren RF. Evaluation of a porous polyurethane scaffold in a partial meniscal defect ovine model. Arthroscopy 2010;26(11):1510–1519.
18. Zur G, Linder-Ganz E, Elsner JJ, Shani J, Brenner O, Agar G, Hershman EB, Arnoczky SP, Guilak F, Shterling A. Chondroprotective effects of a polycarbonate-urethane meniscal implant: Histopathological results in a sheep model. Knee Surg Sports Traumatol Arthrosc 2011;19(2):255–263.
19. Lee CH, Rodeo SA, Fortier LA, Lu C, Erisken C, Mao JJ. Protein-releasing polymeric scaffolds induce fibrochondrocytic differentiation of endogenous cells for knee meniscus regeneration in sheep. Sci Transl Med 2014;6(266):266ra171.
20. Kon E, Filardo G, Tschon M, Fini M, Giavaresi G, Marchesini Reggiani L, Chiari C, Nehrer S, Martin I, Salter DM, Ambrosio L, Marcacci M. Tissue engineering for total meniscal substitution: Animal study in sheep model--Results at 12 months. Tissue Eng Part A 2012;18(15–16):1573–1582.
21. Patel JM, Merriam AR, Kohn J, Gatt CJ Jr, Dunn MG. Negative outcomes of poly(L-lactic acid) fiber-reinforced scaffolds in an ovine total meniscus replacement model. Tissue Eng Part A 2016;22 (17–18):1116–1125.
22. Holloway JL, Lowman AM, Palmese GR. Mechanical evaluation of poly(vinyl alcohol)-based fibrous composites as biomaterials for meniscal tissue replacement. Acta Biomater 2010;6(12):4716–4724.
23. Yang F, Murugan R, Wang S, Ramakrishna S. Electrospinning of nano/micro scale poly(L-lactic acid) aligned fibers and their potential in neural tissue engineering. Biomaterials 2005;26(15):2603–2610.

24. Sarkar S, Lee GY, Wong JY, Desai TA. Development and characterization of a porous micro-patterned scaffold for vascular tissue engineering applications. Biomaterials 2006;27(27):4775–4782.
25. Xie J, Li X, Lipner J, Manning CN, Schwartz AG, Thomopoulos S, Xia Y. "Aligned-to-random" nanofiber scaffolds for mimicking the structure of the tendon-to-bone insertion site. Nanoscale 2010;2(6): 923–926.
26. Lee CH, Shin HJ, Cho IH, Kang YM, Kim IA, Park KD, Shin JW. Nanofiber alignment and direction of mechanical strain affect the ECM production of human ACL fibroblast. Biomaterials 2005;26(11): 1261–1270.
27. Teh TKH, Toh SL, Goh JCH. Aligned hybrid silk scaffold for enhanced differentiation of mesenchymal stem cells into ligament fibroblasts. Tissue Eng Part C Methods 2011;17(6):687–703.
28. Balint E, Gatt CJ Jr, Dunn MG. Design and mechanical evaluation of a novel fiber-reinforced scaffold for meniscus replacement. J Biomed Mater Res A 2012;100(1):195–202.
29. Baker BM, Mauck RL. The effect of nanofiber alignment on the maturation of engineered meniscus constructs. Biomaterials 2007;28 (11):1967–1977.
30. Warren PB, Huebner P, Spang JT, Shirwaiker RA, Fisher MB. Engineering 3D-bioplotted scaffolds to induce aligned extracellular matrix deposition for musculoskeletal soft tissue replacement. Connect Tissue Res 2016;58:1–13.
31. Brophy RH, Cottrell J, Rodeo SA, Wright TM, Warren RF, Maher SA. Implantation of a synthetic meniscal scaffold improves joint contact mechanics in a partial meniscectomy cadaver model. J Biomed Mater Res A 2010;92(3):1154–1161.
32. Merriam AR, Patel JM, Culp BM, Gatt CJ, Dunn MG. Successful total meniscus reconstruction using a novel fiber-reinforced scaffold: A 16-and 32-week study in an ovine model. Am J Sports Med 2015;43(10):2528–2537.
33. Patel JM, Merriam AR, Culp BM, Gatt Jr CJ, Dunn MG. One-year outcomes of total meniscus reconstruction using a novel fiber-reinforced scaffold in an ovine model. Am J Sports Med 2016;44(4): 898–907.
34. Patel JM, Ghodbane SA, Brzezinski A, Gatt CJ Jr, Dunn MG. Tissue-engineered total meniscus replacement with a fiber-reinforced scaffold in a 2-year ovine model. Am J Sports Med 2018;46(8): 1844–1856.
35. Rongen JJ, van Tienen TG, van Bochove B, Grijpma DW, Buma P. Biomaterials in search of a meniscus substitute. Biomaterials 2014; 35(11):3527–3540.
36. Bedi A, Kelly NH, Baad M, Fox AJS, Brophy RH, Warren RF, Maher SA. Dynamic contact mechanics of the medial meniscus as a function of radial tear, repair, and partial meniscectomy. J Bone Joint Surg Am Vol 2010;92A(6):1398–1408.
37. Ghodbane SA, Dunn MG. Physical and mechanical properties of cross-linked type I collagen scaffolds derived from bovine, porcine, and ovine tendons. J Biomed Mater Res A 2016;104(11):2685–2692.
38. Patel JM, Jackson RC, Schneider GL, Ghodbane SA, Dunn MG. Carbodiimide cross-linking counteracts the detrimental effects of gamma irradiation on the physical properties of collagen-hyaluronan sponges. J Mater Sci Mater Med 2018;29(6):75.
39. Kakkar P, Verma S, Manjubala I, Madhan B. Development of keratin-chitosan-gelatin composite scaffold for soft tissue engineering. Korean J Couns Psychother 2014;45:343–347.
40. Mow VC, Kuei SC, Lai WM, Armstrong CG. Biphasic creep and stress relaxation of articular cartilage in compression? Theory and experiments. J Biomech Eng 1980;102(1):73–84.
41. Rimmer MG, Nawana NS, Keene GC, Pearcy MJ. Failure strengths of different meniscal suturing techniques. Arthroscopy 1995;11(2): 146–150.
42. Von Lewinski G, Stukenborg-Colsman C, Ostermeier S, Hurschler C. Experimental measurement of tibiofemoral contact area in a meniscectomized ovine model using a resistive pressure measuring sensor. Ann Biomed Eng 2006;34(10):1607–1614.
43. Zaffagnini S, Grassi A, Marcheggiani Muccioli GM, Bonanzinga T, Nitri M, Raggi F, Ravazzolo G, Marcacci M. MRI evaluation of a collagen meniscus implant: A systematic review. Knee Surg Sports Traumatol Arthrosc 2015;23(11):3228–3237.
44. De Groot J, Zijlstra F, Kuipers H, Pennings A, Klompmaker J, Veth R, Jansen H. Meniscal tissue regeneration in porous 50/50 copoly (L-lactide/ε-caprolactone) implants. Biomaterials 1997;18(8): 613–622.
45. Sandmann GH, Adamczyk C, Grande Garcia E, Doebele S, Buettner A, Milz S, Imhoff AB, Vogt S, Burgkart R, Tischer T. Biomechanical comparison of menisci from different species and artificial constructs. BMC Musculoskelet Disord 2013;14:324.
46. Richards C, Gatt C, Langrana N, Calderon R. Quantitative measurement of human meniscal strain. Trans Orthop Res Soc 2003;28:649.
47. Arnoczky SP, Warren RF. Microvasculature of the human meniscus. Am J Sports Med 1982;10(2):90–95.
48. Chevrier A, Nelea M, Hurtig MB, Hoemann CD, Buschmann MD. Meniscus structure in human, sheep, and rabbit for animal models of meniscus repair. J Orthop Res 2009;27(9):1197–1203.
49. Beamer BS, Masoudi A, Walley KC, Harlow ER, Manoukian OS, Hertz B, Haeussler C, Olson JJ, Deangelis JP, Nazarian A, Ramappa AJ. Analysis of a new all-inside versus inside-out technique for repairing radial meniscal tears. Arthroscopy 2015;31(2): 293–298.
50. Kohn D, Siebert W. Meniscus suture techniques: A comparative biomechanical cadaver study. Arthroscopy 1989;5(4):324–327.
51. Li S-T, Rodkey WG, Yuen D, Hansen P, Steadman JR. Type I collagen-based template for meniscus regeneration. Tissue Engineering and Biodegradable Equivalents. Scientific and Clinical Applications; New York: Marcel Dekker; 2002. pp. 237–266.
52. Hardeman F, Corten K, Mylle M, Van Herck B, Verdonk R, Verdonk P, Bellemans J. What is the best way to fix a polyurethane meniscal scaffold? A biomechanical evaluation of different fixation modes. Knee Surg Sports Traumatol Arthrosc 2015;23(1):59–64.
53. Cottrell JM, Scholten P, Wanich T, Warren RF, Wright TM, Maher SA. A new technique to measure the dynamic contact pressures on the Tibial plateau. J Biomech 2008;41(10):2324–2329.
54. Verma NN, Kolb E, Cole BJ, Berkson MB, Garretson R, Farr J, Fregly B. The effects of medial meniscal transplantation techniques on intra-articular contact pressures. J Knee Surg 2008;21(1):20–26.
55. Seitz AM, Lubomierski A, Friemert B, Ignatius A, Dürselen L. Effect of partial meniscectomy at the medial posterior horn on tibiofemoral contact mechanics and meniscal hoop strains in human knees. J Orthop Res 2012;30(6):934–942.
56. Maher SA, Rodeo SA, Potter HG, Bonassar LJ, Wright TM, Warren RF. A pre-clinical test platform for the functional evaluation of scaffolds for musculoskeletal defects: The meniscus. HSS J 2011; 7(2):157–163.
57. Roos H, Laurén M, Adalberth T, Roos EM, Jonsson K, Lohmander LS. Knee osteoarthritis after meniscectomy: Prevalence of radiographic changes after twenty-one years, compared with matched controls. Arthritis Rheum 1998;41(4):687–693.
58. Smith JP 3rd, Barrett GR. Medial and lateral meniscal tear patterns in anterior cruciate ligament-deficient knees. A prospective analysis of 575 tears. Am J Sports Med 2001;29(4):415–419.
59. Brzezinski A, Ghodbane SA, Patel JM, Perry BA, Gatt CJ, Dunn MG. The ovine model for meniscus tissue engineering: Considerations of anatomy, function, implantation, and evaluation. Tissue Eng Part C Methods 2017;23(12):829–841.
60. Ghodbane SA, Brzezinski A, Patel JM, Pfaff WA, Marzano KN, Gatt CJ, Dunn MG. Partial meniscus replacement with a collagen-hyaluronan infused 3D printed polymeric scaffold. Tissue Eng Part A 2018. https://doi.org/10.1089/ten.TEA.2018.0160